Fuel 268 (2020) 117360

Contents lists available at ScienceDirect

Fuel

journal homepage: www.elsevier.com/locate/fuel

Full Length Article

Study on ignition behaviors of bias parallel pulverized coal streams in a reducing atmosphere: Influences of exit velocity

Guang Zeng[a,b,*], Yijun Zhao[c], Yongtie Cai[a,b], Zhimin Zheng[d], Zhenwei Li[a,b], Mingchen Xu[a,b], Wenming Yang[a,b,*]

[a] Department of Mechanical Engineering, National University of Singapore, 9 Engineering Drive 1, Singapore 117575, Singapore
[b] Sembcorp-NUS Corporate Laboratory, 1 Engineering Drive 2, Singapore 117576, Singapore
[c] School of Energy Science and Engineering, Harbin Institute of Technology, 92, West Dazhi Street, Harbin 150001, PR China
[d] School of Energy and Environment, Anhui University of Technology, 59 Hudong N Road, Huashan, Ma'anshan 243032, PR China

ARTICLE INFO

Keywords:
Bias parallel pulverized coal streams
Low-NO_x combustion technology
Exit velocity
Ignition behaviors
Reducing atmosphere
Indonesian coal

ABSTRACT

Ignition experiments regarding the combustion of Indonesian coal were performed in a reducing atmosphere using a bias combustion simulator with a thermal power of 250-kW. Flame spectra, gas temperatures and gas species were recorded, and coal combustion residues were sampled. The influences of exit velocity on the ignition mechanism, ignition delay distance, continuous flame boundary and fuel NO_x formation of bias parallel pulverized-coal streams were investigated. The experimental results reveal that as exit velocity increased, the peak value of visible-light intensity, the combustion efficiency and the flame stability gradually decreased, while the ignition delay distance, the continuous flame boundary, and the formation of fuel NO*x* gradually increased. Furthermore, the ignition behaviors became worse. A transition of ignition mechanism occurred with increasing exit velocity, at an exit velocity of 16 m/s, the bias parallel pulverized-coal streams ignited in a hetero-homogeneous joint mechanism; at exit velocities of 20, 25 and 29 m/s, the bias parallel pulverized-coal streams ignited in a homogeneous mechanism. For different exit velocities, the fuel-rich stream ignited in advance of the fuel-lean stream, and the continuous flame boundary leaned evidently towards the fuel-rich stream side. According to the experimental findings in the present study, the horizontal bias combustion pulverized-coal burners were designed and applied to one-sixth of the total burners in a tangentially-fired pulverized-coal boiler. At the rated electrical load of 500 MW*e*, the NO_x concentration prior to denitrification decreased by 11%, and the ammonium consumption for denitrification decreased by 42 kg/h. The results of the present study are also beneficial to further advance ignition concepts of low NO_x bias combustion of pulverized-coal and enable the related numerical simulation work.

1. Introduction

Coal's share in power generation is still at 38% and accounts for the largest percentage [1]. Indonesian coal is widely used in the world due to the low price of the coal and good accessibility of shipment, as well as high demand from countries like China, India, Japan, South Korea, etc. [1]. Tangentially-fired pulverized-coal (PC) boilers are being well modernized, improved and developed around the world [2]. In a tangentially-fired PC boiler, the PC carried by primary air as a PC stream is sent into the boiler through the nozzles of coal burners, meanwhile the secondary air required for combustion is injected into the boiler through the nozzles of secondary air. The horizontal bias combustion (HBC) technique has been extensively applied to the tangentially-fired PC boilers due to its low-NO_x formation and high combustion efficiency. In the HBC technique, the parallel PC streams of fuel-rich and fuel-lean are horizontally injected into the furnace, which are then ignited in an oxygen-deficient atmosphere and an oxygen-rich atmosphere, respectively [3,4]. Air-staged combustion technologies are now being well developed for the PC boilers [5,6], which create an oxygen-deficient combustion environment in the main combustion zone (also referred to as the primary combustion zone) to achieve extremely low-NO_x emission [7,8]. However, if the air-to-coal ratio in the main combustion zone is too low [9]. The complete combustion process will be affected, resulting in a decrease in combustion efficiency [10–13]. Accordingly, in order to guide the rational development of the low-NO_x HBC technique, the ignition behaviors of bias parallel PC streams under

Abbreviations: PC, pulverized-coal; HBC, horizontal bias combustion; EV, exit velocity; BCS, bias combustion simulator

* Corresponding authors at: Department of Mechanical Engineering, National University of Singapore, 9 Engineering Drive 1, Singapore 117575, Singapore.
E-mail addresses: mpezeng@nus.edu.sg (G. Zeng), mpeywm@nus.edu.sg (W. Yang).

https://doi.org/10.1016/j.fuel.2020.117360
Received 2 November 2019; Received in revised form 24 December 2019; Accepted 7 February 2020
Available online 21 February 2020
0016-2361/

a reducing environment need to be further investigated.

Ignition plays an extremely significant role in the design of the combustor and burner as well as in the combustion process itself. Numerous studies have been conducted on the ignition mechanism, ignition delay, flame stability and combustion characteristics, etc. [14–16]. There are three well-known ignition mechanisms of coal, i.e., heterogeneous, gas-phase or homogeneous, and hetero-homogeneous joint ignition [17,18]. Khatami et al. revealed that the coal particle combustion was categorized into one-mode and two-mode, i.e., simultaneous ignition of the char and volatile and sequential ignition of volatiles and char [15,19,20]. Generally, the ignition of a PC stream can be classified into three regions of preheating, growing flame and continuous flame. Accordingly, two kinds of delay distances were introduced. One is defined as the ignition delay distance from the starting point of PC stream to the onset of the growing flame. The other is defined as the continuous flame delay distance from the starting point of PC stream to the onset of the continuous flame [21–23]. Even so, the detailed ignition behaviors of bias parallel PC streams in a tangentially-fired PC boiler remain inadequately understood due to the complexity of the experimental facility.

The primary air velocity in a coal-fired boiler is the exit velocity (EV) of a PC stream at the burner nozzle, which is critical to the stability and safety of the combustion. There will be a stable ignition delay distance if the imposed primary air velocity matches the flame velocity (rate of burning); otherwise there may be flame blow off or flash back [23]. In a tangentially-fired PC boiler, appropriately designed EV for a PC burner burning a coal with different ignition behaviors is not only suitable for optimizing combustion performance, but also important for the pollutant emission [24]. Regrettably, the selection of EV for a PC burner burning a new coal mostly depends on experience rather than an experimental investigation [25]. Our previous experimental study revealed that there was an optimal EV at which the ignition characteristics of bias parallel PC streams were the best [25]. It can be seen that the EV can severely affect the ignition of PC, and consequentially affect the NO_x formation characteristics of bias parallel PC streams, which was not studied in our previous publication [25]. The further study of the influences of EV on the NO_x formation characteristics in the ignition stage of bias parallel PC streams will bring more environmental and economic benefits to the tangentially fired PC boilers burning a new coal. Xu et al. studied the ignition of a PC stream in an entrained flow reactor, using a camera to record the flame characteristics [16]. The results indicated that as EV increased, the ignition distance decreased, and the flame of PC stream became wide and turbulent. Zhang et al. investigated the effects of primary air and secondary air on the ignition of a turbulent PC stream under an oxy-combustion environment [26]. However, the results obtained using these experimental means evidently differ from the results obtained in the furnaces of actual tangentially-fired PC boilers [23]. Consequently, it is extremely necessary to design an appropriate experimental setup to further study the influences of EV on the ignition behaviors of bias parallel PC streams in tangentially fired PC boilers, with the purpose of benefiting the advantages of HBC technique.

Numerous experimental setups have been used for the research of coal combustion. Zeng et al. performed coal combustion experiments in a Hencken burner, using an optical fiber spectrometer and a camera, to investigate the behaviors of coal particles burning under oxy-coal combustion conditions [27]. Adeosun et al. employed a two-stage Hencken burner with digital videography, to identify the ignition delay distance and ignition mode of coal particle in a reducing-to-oxidizing atmosphere [28,29]. Nonetheless, the PC stream in the above-mentioned studies was heated by only the plane temperature distribution in the experimental setups [16,27–31]. Likewise, drop tube furnaces or other reactors were also applied to investigate the PC ignition behaviors, but the main heat transfer mode in the electrical heating furnace was radiation, which was not the same as the convection heat transfer in the actual boilers. Besides, the flow characteristics in these experimental setups also differed from the tangentially-fired PC boilers [15,19,20,32–34]. Moreover, the coal mixed with the high-temperature gas was tested in some vertical or horizontal furnace reactors. Dobó et al. conducted pilot-scale experiments in a high-pressure down-fired combustor, using multiple measurements to investigate the operational performance of coal-water slurry under the oxy-combustion conditions [35]. Clements et al. performed the pilot-scale experiments in a horizontal furnace combustion facility to study ignition behaviors of mixed fuel of coal and petroleum coke [36]. Evidently, these researches have only concentrated on the combustion behaviors of single PC stream, without adequately clarifying the ignition process of PC bias combustion in a tangentially-fired PC boiler [26,35–37]. Correspondingly, the results revealed in the aforementioned experiments are conducive to understanding and analyzing the ignition of the conventional PC stream but are inadaptable to the research of the ignition of two bias parallel PC streams in tangentially-fired PC boilers.

The bias combustion simulator (BCS) with the thermal power of 250-kW was used in the present study and was capable of simulating the ignition state of a straight jet burner at one corner of an actual tangentially-fired PC boiler. Compared with other experimental facilities, in an accurate and flexible way, the BCS can regulate the flowrate and mixing point of six streams in the main combustion zone, including two bias PC streams, two secondary air streams and two high-temperature flue gases, which is more applicable to the study of the bias combustion in a tangentially-fired PC boiler [3,4,25,38]. The flame fluctuates during the ignition of bias parallel PC streams, the combustion temperature thus fluctuates. These fluctuations, however, cannot be recorded accurately by the thermocouples in a timely manner. It is hence essential to employ an optical method in the experimental setup to observe the fluctuation of the flame [14,28,29,37,39,40]. Except for the traditional measurement methods, the present study collected the flame spectra in the BCS employing a spectrometer. The results of the present study are conducive to the industrial application of the low-NO_x bias combustion technology. Additionally, they can enable relevant numerical simulation of bias parallel PC streams ignition in a reducing atmosphere.

The results are not only helpful to parameter design of the HBC PC burner technology, but also conducive to further advance the ignition theory of low NO_x bias combustion in a reducing atmosphere and enable related numerical simulation work. Additionally, they provide a baseline for the future study of the ignition behaviors of PC bias combustion in an oxygen-enriched condition.

2. Experiment

2.1. Experimental setup

Fig. 1 shows a schematic diagram of the BCS, and the detailed parameters were listed in Table 1. From a forced-draft fan, cold air enters an air preheater for heating. Furthermore, after the temperature has been being regulated by a mixture of hot and cold air in the windboxes, the air with desired temperature is supplied into the pipes of primary air and secondary air, respectively. Two shares of Indonesian coal from two PC silos, after being fed continuously and stably by the variable-frequency screw feeders and mixed with primary air as two bias parallel PC streams, are finally introduced into the main combustion zone to achieve bias combustion condition. The oxygen consumed in the ignition stage is provided by the primary air, and the oxygen required for maintaining a reasonable equivalence ratio of air-to-coal in the BCS is replenished by the secondary air. In a tangentially-fired boiler with HBC PC burners, the fuel-rich stream and fuel-lean steam are ignited by the high temperature flue gases from the fire side and back side, respectively. Accordingly, two high-temperature gases from the complete combustion of propane, are injected into the main combustion zone through two alloy-steel pipes. The gases create an ignition environment simulating that of a tangentially-fired PC boiler. The high-

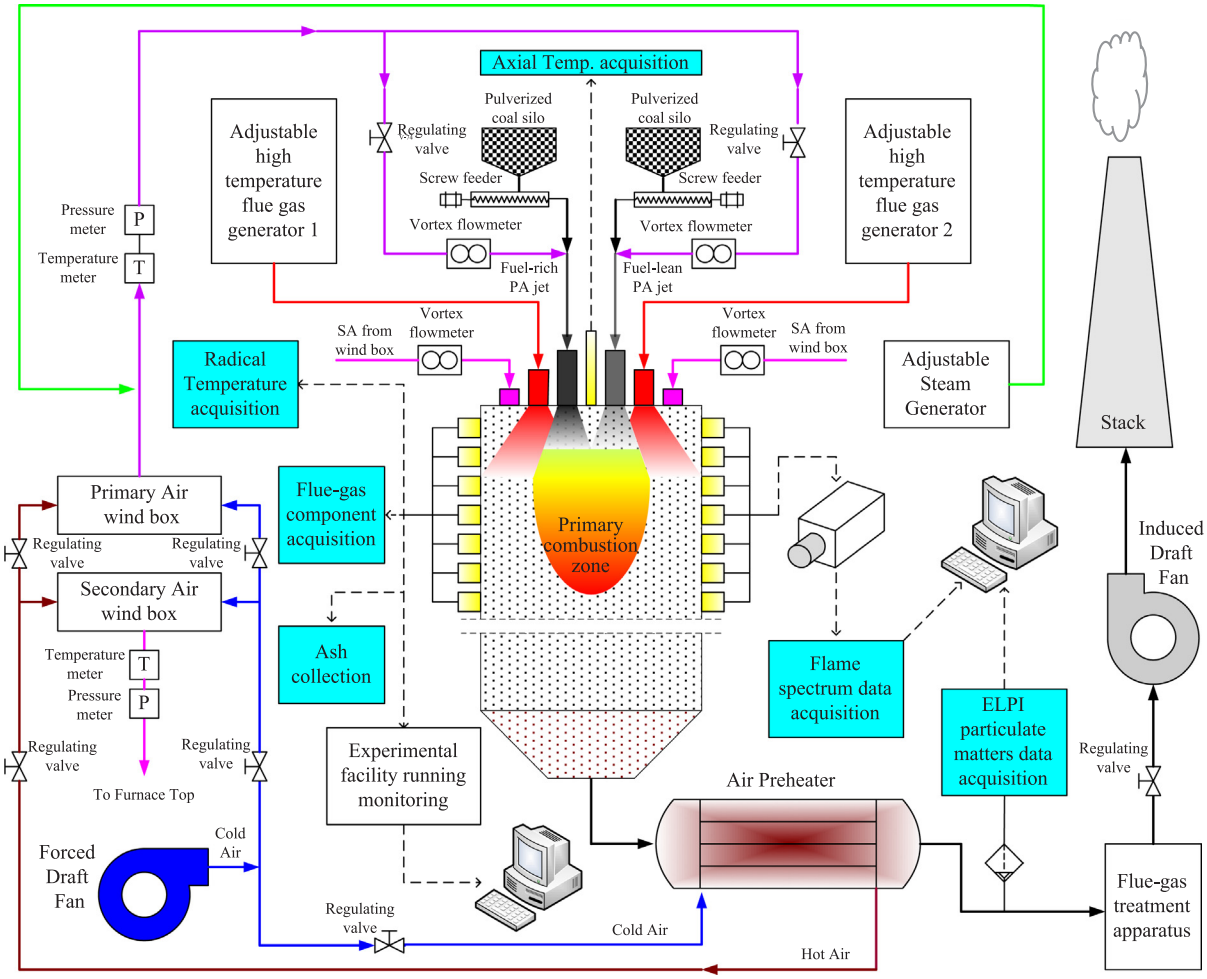

Fig. 1. Schematic diagram of the BCS system.

Table 1
Main parameters of pilot-scale BCS.

Parameter	Value
Rated total thermal power	250 kW
Rated coal fired thermal power	200 kW
Rated gas fired thermal power	50 kW
Coal feeding flow rate	36.778 kg/h
Propane feeding flow rate	2 Nm^3/h
Primary Air/Secondary Air temperature	85/250 °C
Total air flowrate	140.143 Nm^3/h
Maximum operation temperature	1500 °C
Main combustion zone height	1280 mm
Furnace inner diameter	800 mm

temperature gases are used to ignite the bias parallel PC streams and maintain the stable combustion in BCS, which can approximate the ignition state of a bias combustion burner at one corner in a tangentially-fired PC boiler [37]. The detailed arrangement of different streams in the BCS is shown in Fig. 2. The flue gas from the main combustion zone passes through the back-end flue gas ducts and other equipment in sequence, and finally enters the chimney. The airflow and PC bias feeding in the BCS can be flexibly regulated to ensure accurate experimental conditions and stable operation in the experiments [3,4,25,38].

The BCS has a tube furnace with the main combustion zone at the top. There are multiple experimental means in the BCS to record accurate information on the flame spectra, gas species concentrations, coal combustion residues, as well as radial and axial temperatures, as shown in Fig. 1. In the BCS, measurement ports are located on both sides of the main combustion zone at different axial distances vertically from up to bottom. Correspondingly, the flame spectra and images were recorded through the ports on the right side. Meanwhile, through the ports on the left side, a water-cooled stainless steel probe was utilized to obtain the gas species concentrations on-line, while the coal combustion residues were sampled for off-line analysis. The radial temperatures were measured in the horizontal direction along the furnace internal diameter through the left side ports, while the axial temperatures were acquired in the vertical direction along the central axis of the BCS, through a measurement port located in the middle of bias parallel PC streams at the top of the main combustion zone [3,4,25,38].

In the present study, the Inconel armored type-K thermocouples with diameters of 2 mm were used to measure the gas temperatures [19,26,41]. A fiber-optic spectrometer UV–VIS (USB-650 UV) from Ocean Optics was employed to determine the flame characteristics in the main combustion zone of the BCS. Two types of spectral images were collected by the spectrometer. The first was of the scope mode spectra, also referred to as the original spectra, and the second was of the spectra calibrated by absolute irradiance [4,25,38]. The emission intensities of light rays in the two types of spectra increased as temperature increased in the BCS [42]. A VARIO PLUS type MRU flue gas analyzer was used to measure the gas species including NO_x, O_2, CO_2 and CO, which were in the range of 0–300 ppm, 0–3%, 0–14% and 0–500 ppm, respectively. An Indonesian coal from Trafigura was tested in China according to the standard of GB/T 31391-2015. The typical analysis is listed in Table 2, of which the oxygen content was calculated based on the measured results of other components. There was a full

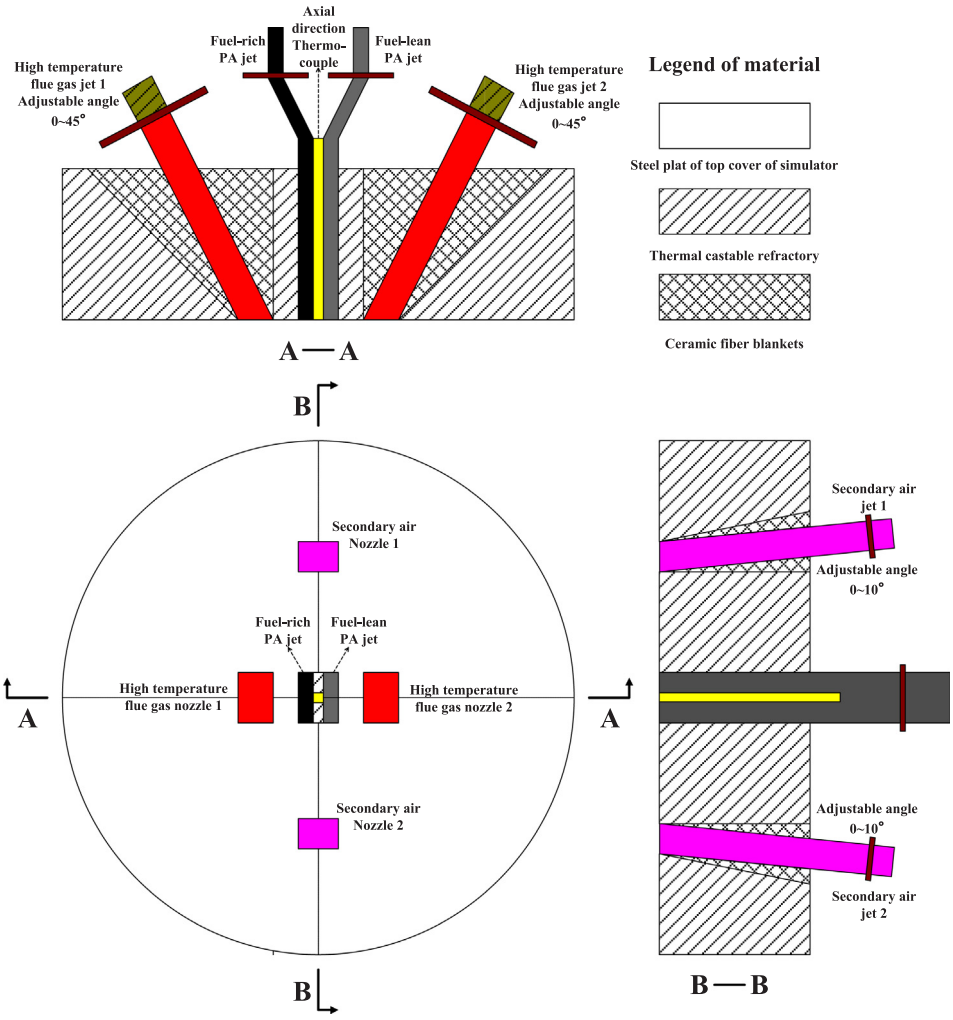

Fig. 2. Schematic of different streams arrangement in the BCS.

particle size distribution for the samples, and the proportion of the particles with a size above 75 μm was 16% [3,4,25,38].

2.2. Experimental methodology

In the experiments performed in the 250-kW BCS, the thermal powers of coal and propane were fixed at 200-kW and 50-kW, respectively. The equivalence ratio between air and coal in the BCS was set at 0.75 for maintaining a reducing atmosphere. The initial coal concentration that is the total mass ratio between coal and air in the PC streams was set at 0.33 kg/kg; the bias concentration ratio that is the coal mass ratio between the streams of fuel-rich and fuel-lean was set at 4; the exit temperatures (or named as initial temperatures) of primary air and secondary air were set at 85 °C and 250 °C, respectively. The bias PC burner exits were set at axial distance of 0 mm in the experiments. The above parameters were validated well in our previous publications [3,25,38]. Four experimental conditions of variable EVs for the PC streams were set at 16, 20, 25 and 29 m/s, respectively, which are commonly used by the tangentially-fired PC boilers. Based on the constant flowrates of primary air and secondary air in this study, the variable EVs were achieved through the replacement of bias PC burners for different experimental conditions, while the secondary air velocity was fixed at 26 m/s. In order to provide the findings beyond a particular geometry, the dimensionless numbers of the bias parallel PC streams are listed in Table 3.

To ensure the reliability and stability, a strict standard operating procedure was implemented in the experiments. When the preset values were reached, the stable experimental condition was determined as follows [3,4,25,38].

(1) The fuel-rich stream and fuel-lean stream were fed stably by the calibrated screw feeders.
(2) The negative pressure at the exit of the furnace was controlled at −100 Pa.
(3) The monitored gas species including NO_x, O_2, CO_2 and CO deviated in the range of 0–1%.

Table 2
Typical sample analysis of the Indonesian coal.

Ultimate (%, as received basis)					Proximate (%, as received basis)				Lower heating value (kJ/kg)
C	H	O	N	S	Fixed carbon	Volatile	Ash	Moisture	
51.77	3.7	15.5	0.85	0.42	36.61	35.63	5.06	22.7	19,508

Table 3
Dimensionless numbers of the bias parallel PC streams.

Reynolds number of EVs				Momentum ratios of air to fuel at different EVs			
16 m/s	20 m/s	25 m/s	29 m/s	16 m/s	20 m/s	25 m/s	29 m/s
19,091	21,727	23,669	25,540	6.17	5.54	5.03	4.75

(4) The measured combustion temperatures deviated within the scope of 0–1% (12 °C).
(5) The fluctuation of the collected flame spectra owing to normal flame pulsation was in the deviation of 0–10%.

In order to ensure the accuracy and repeatability, parameters were recorded only if the experiments could be repeated in the present study. The average value of each parameter was taken to minimize errors. Gas temperatures were recorded automatically by a computer once per minute for a period of ten minutes, and the average temperatures were taken as the final radial and axial temperatures. The two kinds of flame spectra were collected on-line four times per second for thirty seconds. The averages of the selected one hundred spectra were taken as the final spectra for the scope mode spectrum and the spectrum calibrated by absolute irradiance, respectively. The gas species concentrations were measured on-line for 20 times in an experimental case, and the average concentration values were taken as the final value for NO_x, O_2, CO_2 and CO. More details regarding the experimental studies were presented in the relevant publications [3,4,25,38].

In the present study, multiple experimental methods including flame spectra, gas temperatures, the carbon burnouts of coal combustion residues, the volatile burnout and fixed-carbon burnout, as well as the conversion rates from fuel nitrogen to NO_x were analyzed to obtain accurate ignition behaviors of bias parallel PC streams. Prior to two shares of coal being fed into the BCS, the axial blank temperatures were measured when a stable temperature profile was formed in the main combustion zone. All the axial blank temperatures were universal in the experiments [25]. The axial differential temperature of bias parallel PC streams in the BCS was obtained by subtracting axial blank temperature from the axial temperature with coal burning [3,25,38], indicating the trend of heat released from coal during the ignition [15,43,44]. Thereby the ignition mechanism of bias parallel PC streams could be determined firstly according to the reason that one heat release spike represents simultaneous ignition of the char and volatile, and two heat release spikes stands for sequential ignition of volatiles and char [3,25,38]. Moreover, the emission intensities of the volatile and char in the ignition stage were compared using the light rays at the specified wavelengths in the same spectrum calibrated by absolute irradiance. To be specific, the emission intensity of hydrocarbon can represent the combustion intensity of volatile [45–49], and the emission intensity of hot soot can represent the combustion intensity of char [45,47,50], hence the ignition mechanism of the bias parallel PC streams could be confirmed [3,25,38]. Furthermore, based on the off-line analysis of the coal combustion residues sampled in the experiments, the ignition mechanism of bias parallel PC streams was demonstrated by the fixed-carbon burnout and volatile burnout; beyond that, the combustion efficiency of bias parallel PC streams was analyzed by the carbon burnout [3,23,25,38]. The fixed-carbon burnout, volatile burnout and combustion efficiency of coal combustion residues were calculated using formulas (1), (2) and (3), respectively, as follows:

$$BO_{FC} = \left[1 - \frac{FC_i}{FC_0} \times \frac{A_0}{A_i}\right] \times 100 \quad (1)$$

$$BO_V = \left[1 - \frac{V_i}{V_0} \times \frac{A_0}{A_i}\right] \times 100 \quad (2)$$

$$CE = \left[1 - \frac{A_0}{1 - A_0} \times \frac{1 - A_i}{A_i}\right] \times 100 \quad (3)$$

where BO_{FC}, BO_V, and CE (%) are the fixed-carbon burnout, volatile burnout and combustion efficiency, respectively; FC_i, V_i, and A_i (%) are the contents of the fixed carbon, volatile, and ash of the dry sampled coal combustion residues, respectively; and FC_0, V_0, and A_0 (%) are the contents of the fixed carbon, volatile, and ash of the dry coal, respectively [3,23,25,38].

In the present study, the ignition delay distance was investigated accurately using the visible-lights in the scope mode spectra from different experimental cases. The ignition delay distance in the BCS was determined as the distance where the visible-light intensity reached 10% of the spike average value [3,25,30,38,51], which was also validated well with the flame onset location observed in the field of experimental setup [3,25,38]. Normally, a PC stream enters its continuous flame region at the position where the combustion reaches 50% intensity of the maximum value [21,22,48]. Thereby the continuous flame delay distance was determined as the location where the visible-light intensity reached 50% of the spike average value [16,21,22,30,47]. The above defined ignition delay distance and continuous flame delay distance showed the same tendency in the experiments. Moreover, the continuous flame boundary was determined by the continuous flame delay distance and radial temperature distributions [52].

In order to judge the better ignition behaviors of bias parallel PC streams, the criterion was determined as the shorter ignition delay distance, higher combustion efficiency, more intense visible-light, more stable flame, and less formation of fuel NO_x [4,25,38].

3. Results and discussion

3.1. Ignition mechanism of bias parallel PC streams at different EVs

If the char and volatile ignite simultaneously during coal combustion, the rate of heat release will be relatively high with one obvious spike in the axial differential temperatures. If the volatile ignites first without the combustion of char, the rate of heat release will be relatively low with a small spike in the axial differential temperatures. As the char burns afterward, a second large spike will appear in the distribution of the axial differential temperatures [26,43,44,53]. The axial differential temperatures at different EVs for bias parallel PC streams are shown in Fig. 3. It can be seen that the axial differential temperatures gradually increased after an axial distance of 540 mm because the secondary air gradually mixed into the ignition of the bias parallel PC

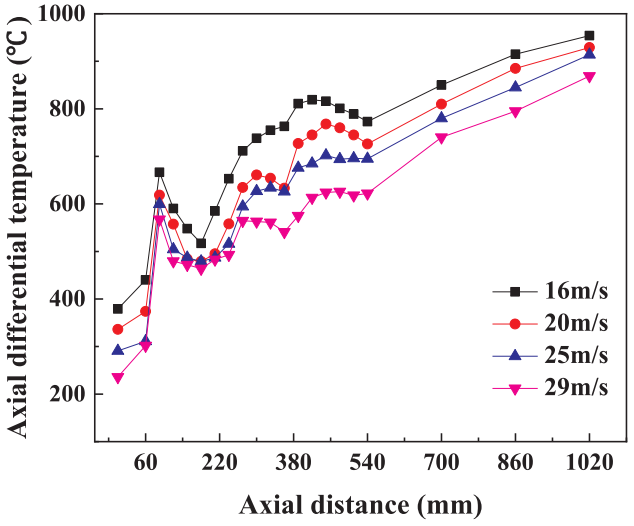

Fig. 3. Axial differential temperatures at different EVs.

streams after 540 mm, which was similar to the actual state in a tangentially-fired PC boiler. Furthermore, the axial differential temperatures have one obvious spike before the 180 mm, which is because two bias PC streams began to intersect and absorb heat at the BCS central axis from the 90 mm. Accordingly, as the two bias PC streams gradually mixed with the two high-temperature gases after the 180 mm, the trend of heat released from the ignition can be reflected by the distribution of axial differential temperatures from 180 to 540 mm [3,25,38]. It is seen that from the 180 to 540 mm, at an EV of 16 m/s, one obvious spike with a pause appears in the distribution of axial differential temperatures. Meanwhile, at EVs of 20, 25 and 29 m/s, two obvious spikes appear in the axial differential temperatures, with the second spikes being larger than the first.

The single spike in the axial differential temperatures at an EV of 16 m/s arose from the heat released from the simultaneous ignition of the chars and volatiles [20,32,33], which preliminarily indicates that the bias parallel PC streams at an EV of 16 m/s ignited in a char-volatile joint mode [3,20,25,32,33,38]. At EVs of 20, 25 and 29 m/s, the first spikes in the axial differential temperatures arose from the heat released from the ignition of the volatile, and the second spikes arose from the heat released from the ignition of the char [20,32,33,54], which preliminarily indicates that the bias parallel PC streams at EVs of 20, 25 and 29 m/s ignited in a volatile-phase mode [3,20,25,32,33,38,54]. Besides, if the combustion of bias parallel PC streams was more intense, the peak value in the axial differential temperatures would be larger [55]. It is seen that with increasing EV prior to 540 mm, the temperature at the spike of the axial differential temperatures gradually decreased, demonstrating that the intensity of bias parallel PC streams combustion gradually decreased.

In contrast to 16 m/s, at higher EVs of 20, 25 and 29 m/s, the bias parallel PC streams absorbed less radiation heat from the surroundings owing to the fact that less time was taken at the same distance, resulting in the ahead ignition of volatile. Afterward, the bias parallel PC streams continuously absorbed more convection heat from high-temperature gases owing to greater turbulence intensities at higher velocities, leading to the subsequent combustion of char.

The ignition mechanism of bias parallel PC streams can be further confirmed based on the emission intensities of hot soot and hydrocarbon in the flame spectra. The absolute irradiances of hot soot and hydrocarbon at different EVs for bias parallel PC streams are shown in Figs. 4–7. It is observed that the spike positions of absolute irradiances of hot soot and hydrocarbon gradually increased as EV increased, which were at 700 mm for EVs of 16 and 20 m/s, respectively, 860 mm for an EV of 25 m/s and 1020 mm for an EV of 29 m/s. Figs. 4–7 also demonstrate that the value at the spike of absolute irradiances of hot soot and hydrocarbon gradually decreased with increasing EV, which indicates a gradual decrease in the intensity of bias parallel PC streams combustion.

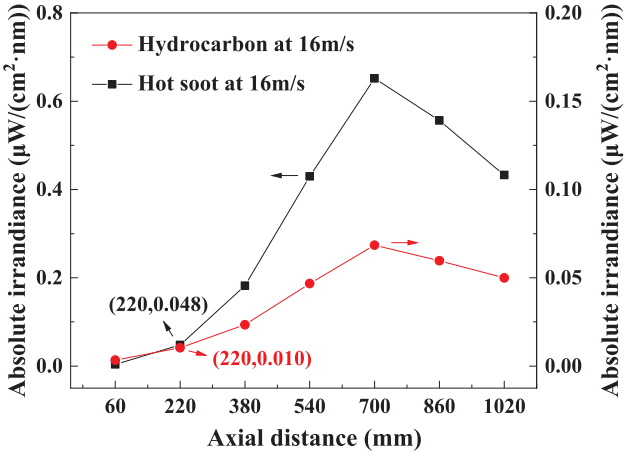

Fig. 4. Axial absolute irradiances of hot soot and hydrocarbon at an EV of 16 m/s.

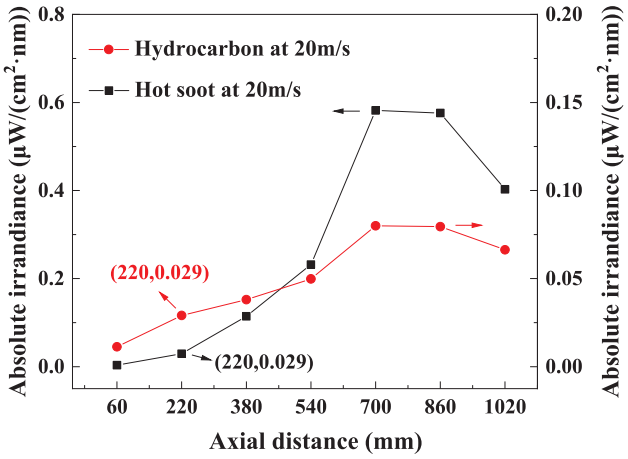

Fig. 5. Axial absolute irradiances of hot soot and hydrocarbon at an EV of 20 m/s.

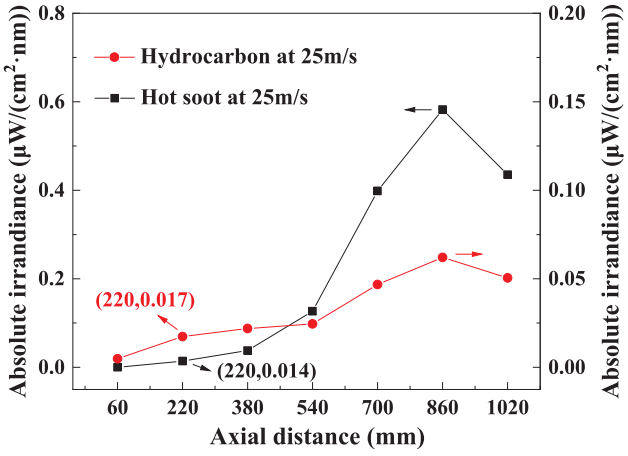

Fig. 6. Axial absolute irradiances of hot soot and hydrocarbon at an EV of 25 m/s.

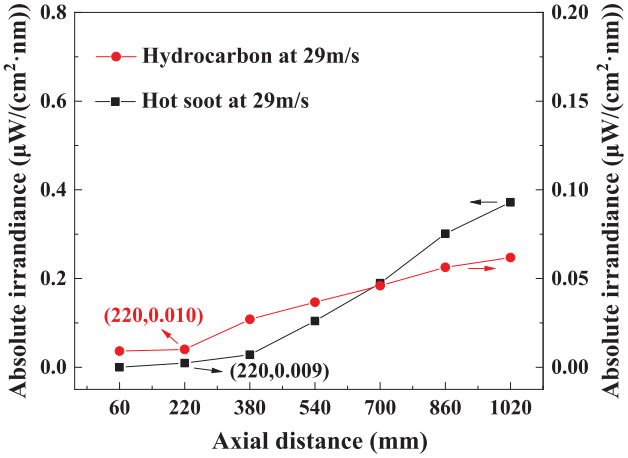

Fig. 7. Axial absolute irradiances of hot soot and hydrocarbon at an EV of 29 m/s.

Fig. 4 shows that at 220 mm in the initial ignition stage, the absolute irradiances of hot soot at an EV of 16 m/s was higher than those of hydrocarbon, which means that the ignition of volatile was not dominant, i.e., the char and volatile of bias parallel PC streams ignited

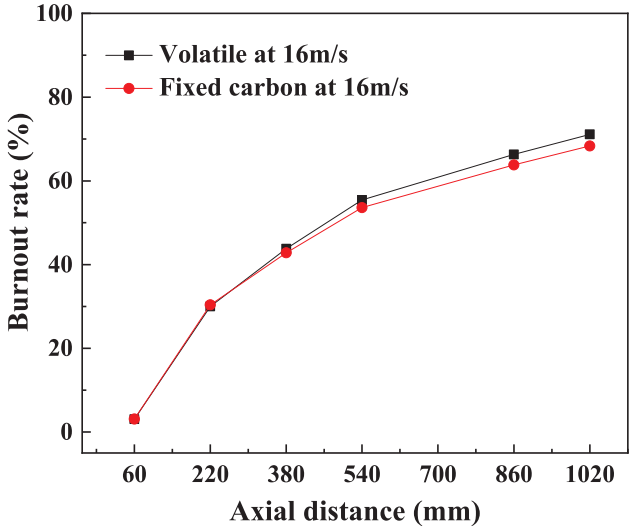

Fig. 8. Volatile burnout and fixed-carbon burnout at an EV of 16 m/s.

simultaneously [19,33]. Hence, the analysis according to flame spectra confirms that the bias parallel PC streams at an EV of 16 m/s ignited in a hetero-homogeneous joint mechanism [3,19,25,33,38], which is consistent with the findings concluded from the axial differential temperatures. Figs. 5–7 show that at 220 mm in the initial ignition stage, the absolute irradiances of hot soot at EVs of 20, 25 and 29 m/s, respectively, were no more than the corresponding values of hydrocarbons, which indicates that the ignition of volatile was dominant, i.e., the volatile and char of bias parallel PC streams ignited successively [19,33]. Therefore, the analysis according to flame spectra confirms that the bias parallel PC streams at EVs of 20, 25 and 29 m/s ignited homogenously [3,19,25,33,38], which is also in good agreement with the findings concluded from the axial differential temperature.

According to the coal combustion residues sampled in the experiments, the volatile burnout and fixed-carbon burnout were used to demonstrate the ignition mechanism of bias parallel PC streams [56–59], as shown in Figs. 8 and 9. At EVs of 16 and 20 m/s, the variation tendencies were similar in that the volatile burnout and fixed-carbon burnout gradually increased as axial distance increased. However, it can be found that at an EV of 16 m/s, the fixed-carbon burnout remained close to volatile burnout prior to 220 mm, demonstrating that the char and volatile ignited simultaneously [25,56–59]; while at an EV

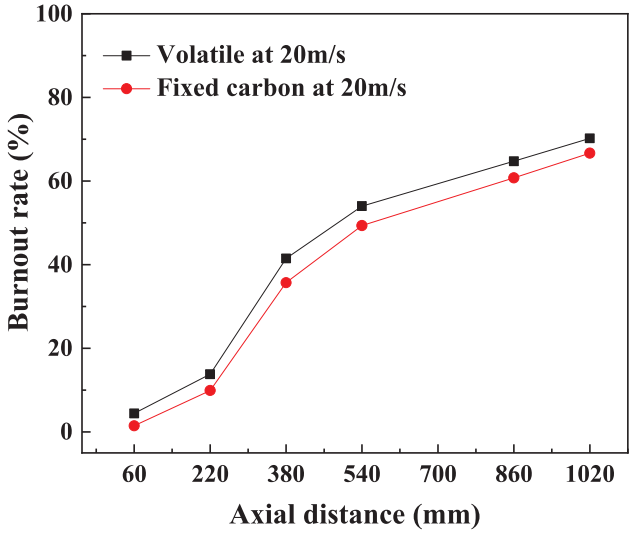

Fig. 9. Volatile burnout and fixed-carbon burnout at an EV of 20 m/s.

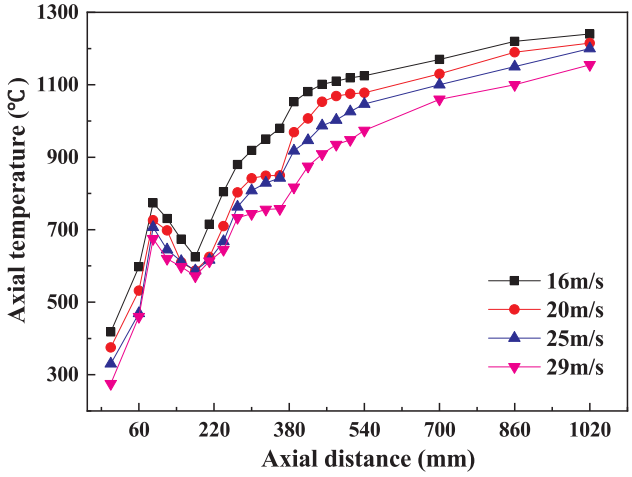

Fig. 10. Axial temperatures at different EVs.

of 20 m/s, the volatile burnout was greater than the fixed-carbon, demonstrating the ahead ignition of volatile [25,56–59]. The findings indicate that when the EV of bias parallel PC streams decreased from 20 m/s to 16 m/s, a transition of mechanism from homogeneous to hetero-homogeneous joint ignition occurred. The ignition mechanism concluded from the volatile burnout and the fixed carbon burnout, as well as the flame spectra were in good agreement with that concluded from the axial differential temperatures.

3.2. Ignition delay distance of bias parallel PC streams at different EVs

Fig. 10 shows the axial temperatures at different EVs for bias parallel PC streams. Similar to the axial differential temperatures displayed above, as the two bias PC streams gradually mixed with the two high-temperature gases, the axial temperatures dramatically increased in the axial distance from 180 to 380 mm, which reveals that the two bias PC streams at different EVs ignited between 180 and 380 mm [25,38]. Furthermore, the increasing rate of axial temperatures was higher at smaller EV, which was because the parallel PC streams absorbed more radiation heat from hot surroundings at smaller velocity [16,23,44]; while at higher EVs, although the parallel PC streams absorbed more convection heat from high-temperature gases, it was extremely limited owing to the little increase in turbulence intensity, indicating that the heat transfer of radiation played a more significant role than that of convection in the initial ignition stage [25].

Fig. 11 shows the visible-light intensities at different EVs for bias parallel PC streams. It can be found that the peak of visible-light intensity was lower at higher EV, indicating that the flame stability gradually decreased as EV increased [3,25,38]. Fig. 12 shows the ignition delay distances at different EVs for bias parallel PC streams. Considering that the maximum axial visible-light intensity might locate either side of the measuring position where the existing spike of visible-light was collected, all ignition delay distances are figured with relative error bars to indicate the uncertainties [3,25,38]. It is seen that the ignition delay distance gradually increased as EV increased. This is because as EV increased, the decrement of radiation heat transfer was greater than the increment of convection heat transfer, which also indicates that the heat transfer of radiation played a more important role than that of the convection during the initial ignition [25].

3.3. Continuous flame boundaries of bias parallel PC streams at different EVs

Distributions of radial temperatures at different EVs for bias parallel PC streams are shown in Figs. 13–16. It can be observed that for the bias parallel PC streams, the radial temperatures at the −20 and +20 mm

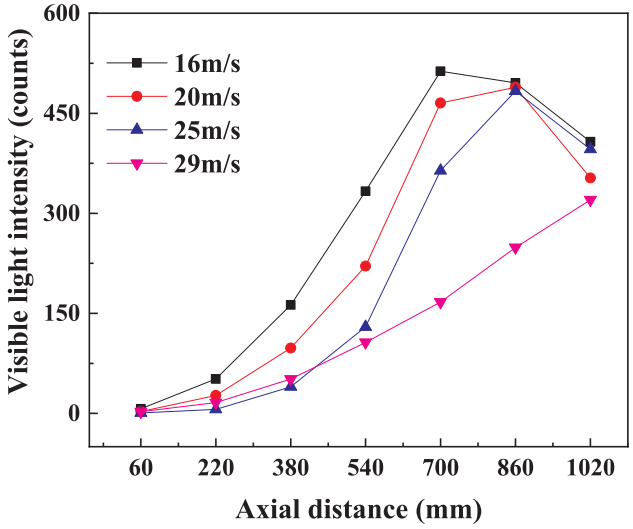

Fig. 11. Axial visible-light intensities at different EVs.

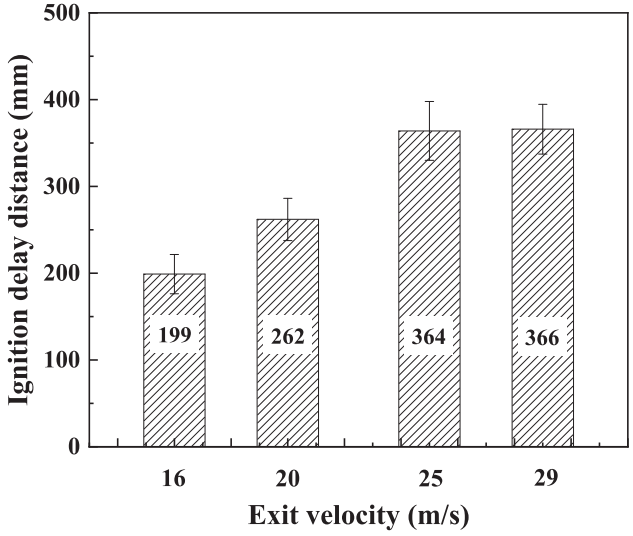

Fig. 12. Ignition delay distances at different EVs.

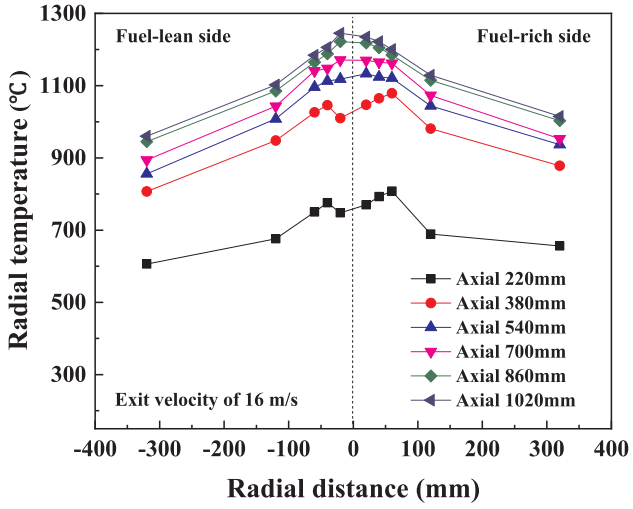

Fig. 13. Distribution of radial temperatures at an EV of 16 m/s.

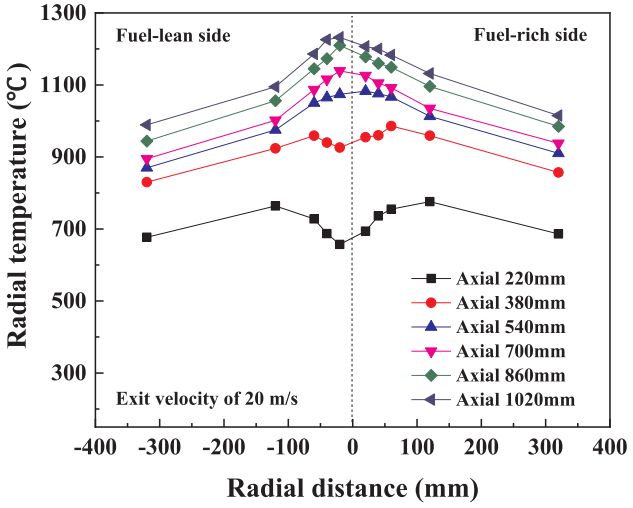

Fig. 14. Distribution of radial temperatures an EV of 20 m/s.

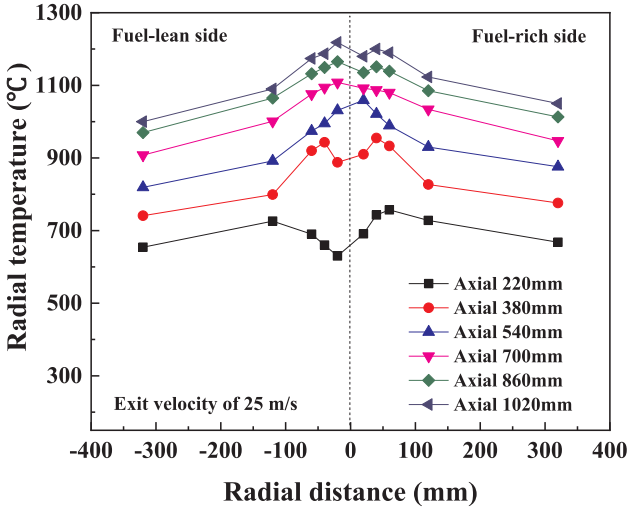

Fig. 15. Distribution of radial temperatures at an EV of 25 m/s.

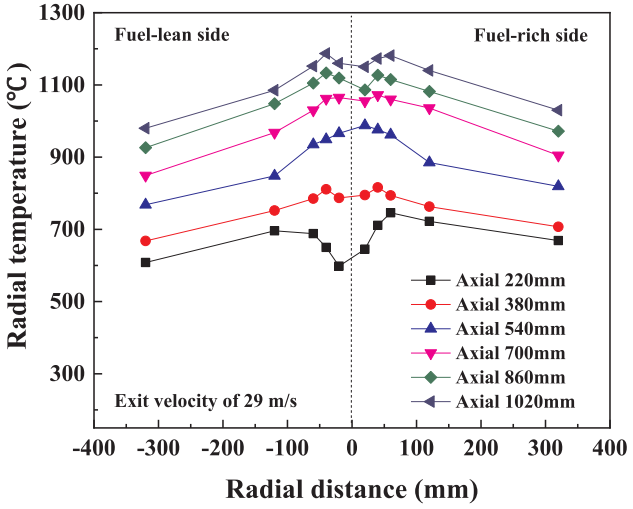

Fig. 16. Distribution of radial temperatures at an EV of 29 m/s.

were first lower than those at the peripheral parts. As axial distance increased, the radial temperatures in the interior became higher than those at the two sides, indicating that the bias parallel PC streams ignited at the edges in the upstream due to that the exchange of mass and heat started at the boundaries, and subsequently spread into the interior owing to continuous exchange of mass and heat in the downstream [25,37,38].

Figs. 13–16 show that for the bias parallel PC streams at different EVs, respectively, the radial temperatures at fuel-rich stream were higher than those at fuel-lean stream at 220 mm, indicating that the fuel-rich stream ignited in advance of the fuel-lean stream in the present study, which means that the EV from 16 m/s to 29 m/s was able to benefit the advantages of HBC technique. It can also be found that the radial temperatures at different EVs gradually increased as axial distance increased, but the temperatures in the fuel-lean stream became higher than that in the fuel-rich stream from 700 mm. This is because in the reducing atmosphere of the BCS with an equivalence ratio of 0.75, oxygen in the fuel-rich stream was mostly consumed during the initial ignition stage, which caused the subsequent combustion of the fuel-lean stream became stronger than that of the fuel-rich stream [25,38]. Besides, at the EVs of 25 and 29 m/s, the radial temperatures in the central part of bias parallel PC streams became lower than that in the peripheral part after 860 mm. The reason was that the ignition delay distances at higher EVs of 25 and 29 m/s were too long, resulting in a delayed combustion at the center of the bias parallel PC streams.

Table 4 shows the continuous flame delay distances and stable ignition temperatures at different EVs [3,25,38,60]. It can be found that with an increase in the EV, the continuous flame delay distance gradually increased, and the stable ignition temperature gradually decreased, indicating that the flame stability gradually decreased.

Based on the distributions of radial-temperatures and stable-ignition temperatures, the temperature boundaries of the continuous flame regions were determined in the present study. Fig. 17 shows the continuous flame boundaries at different EVs for bias parallel PC streams. It is seen that the continuous flame boundaries at EVs of 20, 25 and 29 m/s started at 700 mm and that at an EV of 16 m/s started at 540 mm, due to the fact that the parallel PC streams ignited at an EV of 16 m/s ahead of that at EVs of 20, 25, and 29 m/s. The continuous flame boundary became wider with increasing EV, indicating that the flame stability gradually decreased [25], which is consistent with the previous findings concluded from the flame spectra. It can also be observed that the continuous flame boundaries leaned evidently towards the fuel-rich stream side at different EVs, owing to the ignition of fuel-lean stream in the present study being worse than that of the fuel-rich stream [3,25,38].

3.4. NO_x formation characteristics of bias parallel PC streams at different EVs

Fig. 18 shows the carbon burnouts of coal combustion residues of bias parallel PC streams at EVs of 16 and 20 m/s. The variation tendencies at EVs of 16 and 20 m/s were similar in that the carbon burnouts gradually increased as axial distance increased. Nonetheless, the carbon burnout was higher at an EV of 16 m/s than that at an EV of 20 m/s. Hence, the combustion efficiencies of bias parallel PC streams at different EVs were analyzed by the carbon burnouts of coal combustion residues collected at 380 mm, as shown in Fig. 19. As EV

Table 4
Stable ignition parameters at different EVs.

Item	Value			
Exit velocity (m/s)	16	20	25	29
Continuous flame delay distance (mm)	470	556	615	680
Stable ignition temperature (°C)	1107	1084	1070	1048

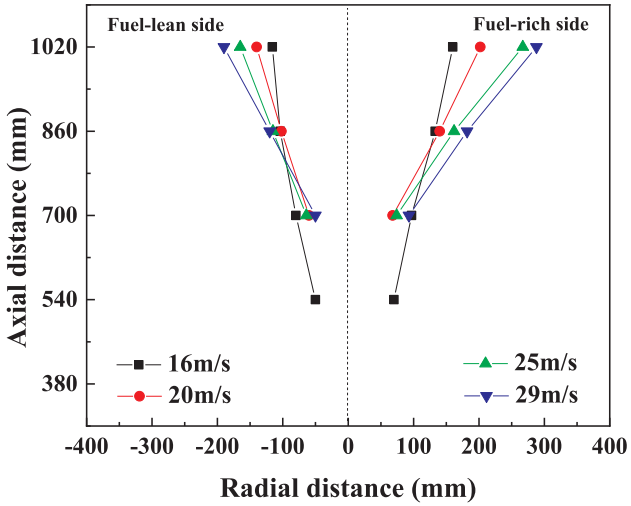

Fig. 17. Continuous flame boundaries at different EVs.

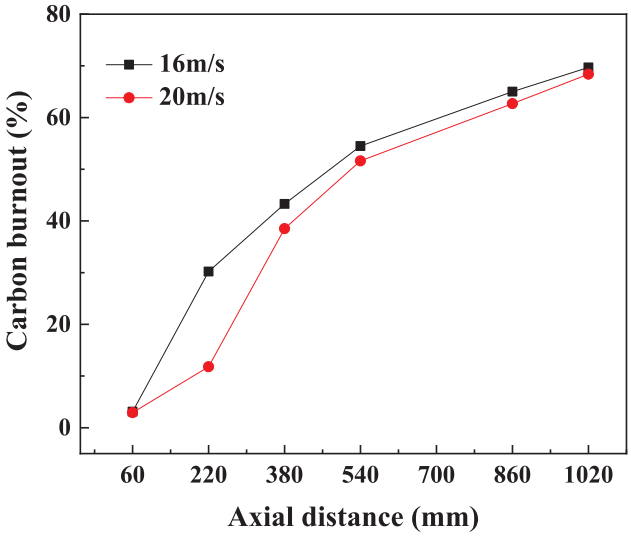

Fig. 18. Carbon burnouts of coal combustion residues at EVs of 16 and 20 m/s.

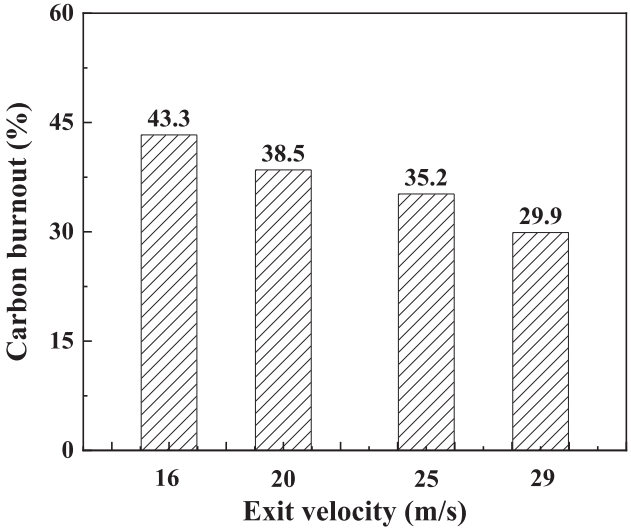

Fig. 19. Carbon burnouts of coal combustion residues at different EVs.

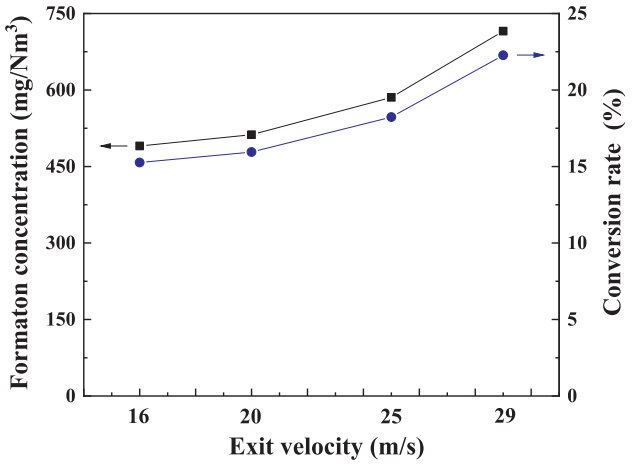

Fig. 20. Formation concentrations and conversion rates of fuel NO_x at different EVs.

increased, the carbon burnout of coal combustion residues gradually decreased, indicating that the combustion efficiency gradually decreased, which agrees well with the findings concluded from the axial differential temperatures and flame spectra [3,25,38].

Most of the nitrogen oxides generated during the PC combustion are fuel NO_x. The conversion rate of fuel NO_x was calculated using formula (4), as follows:

$$CR = \frac{0.14 \times NO_x \times V_y}{22.4 \times N_{ad}} \quad (4)$$

where CR (%) is the conversion rate of fuel NO_x; NO_x (mg/Nm^3, O_2 of 6%) is the NO_x concentration at the outlet of main combustion zone; V_y (Nm^3/kg) is the theoretical dry air volume required per kilogram of coal combustion; N_{ad} (%) is the nitrogen content of coal as air dried basis [61].

Fig. 20 shows that the formation concentrations and conversion rates of fuel NO_x at different EVs for bias parallel PC streams. As EV increased, the concentration of generated fuel NO_x gradually increased. Figs. 19 and 20 show that for bias parallel PC streams at different EVs, the lower the combustion efficiency, the higher the fuel NO_x formation. The main reason was that in an oxygen-deficient atmosphere, if the bias PC streams burned more intensely in the main combustion zone, more oxygen would react with the hydrocarbon and fixed-carbon during the initial ignition stage, which took place in the vicinity of the burner nozzle. Considering that the equivalence ratio between air and coal in the BCS was only 0.75 and far less than 1.0, it would be more difficult for the NO_x precursors released from the Indonesian coal to react with the insufficient oxygen, leading to a lower formation of fuel NO_x [62], which differs from the NO_x formation characteristics in the coal combustion in an oxidizing atmosphere [38].

According to the experimental findings in the present study, the ignition behaviors of bias parallel PC streams were better at EVs of 16 and 20 m/s, which had better combustion efficiency and less NO_x formation compared to those at EVs of 25 and 29 m/s. Accordingly, the recommended range for the EV of the HBC PC burner burning the same Indonesian coal is 16–20 m/s. Finally, in the first phase of industrial application, four HBC PC burners with an EV of 18.5 m/s were designed and applied to one-sixth of the total burners in a tangentially-fired PC boiler in South Korea. When the boiler was running at the rated electrical load of 500 MW*e* with twenty burners in service, in contrast to the original operation condition, the boiler combustion efficiency was maintained the same as before, but the NO_x formation concentration prior to denitrification device decreased by 11% from 265 mg/Nm^3 to 236 mg/Nm^3, and the ammonium consumption for the denitrification decreased by 42 kg/h. Furthermore, in the second phase of industrial application, at least two fifths of the remaining burners in the tangentially-fired PC boiler will be changed to the HBC PC burners which were all designed based on the experimental findings in the present study [63].

4. Conclusions

Ignition experiments were carried out in a BCS at a thermal power of 250-kW. The ignition behaviors of bias parallel PC streams of Indonesian coal at different EVs in a reducing atmosphere were investigated based on the flame spectra and other multiple methods. The major findings are concluded as follows:

As EV increased for the PC streams, the peak value of visible-light intensity, the combustion efficiency and the flame stability gradually decreased while the ignition delay distance, the continuous flame boundary and the formation of fuel NO*x* gradually increased. Furthermore, the ignition behaviors became worse as well as the energy conversion and environmental characteristics became worse.

A transition of ignition mechanism occurred with increasing EV for the bias parallel PC streams. At an EV of 16 m/s, the bias PC streams ignited in a hetero-homogeneous joint mechanism. At EVs of 20, 25 and 29 m/s, the bias PC streams ignited in a homogeneous mechanism.

At different EVs, the bias parallel PC streams ignited at the edges in the upstream and subsequently spread into the interior in the downstream. The fuel-rich stream ignited in advance of the fuel-lean stream, and the continuous flame boundary leaned evidently towards the fuel-rich stream side. However, in an oxygen-deficient atmosphere, the subsequent combustion of the fuel-lean stream became stronger than that of the fuel-rich stream.

According to the experimental findings in the present study, the recommended range for the EV of the HBC PC burner burning the Indonesian coal is 16–20 m/s. Four HBC PC burners with an EV of 18.5 m/s were designed and applied to one-sixth of the total burners in a tangentially-fired PC boiler in South Korea. When the boiler was running with twenty burners in service at the rated electrical load of 500 MW*e*, in contrast to the original operation condition, the boiler combustion efficiency was maintained the same as before, but the NO_x formation concentration prior to denitrification decreased by 11%, and the ammonium consumption for the denitrification decreased by 42 kg/h.

CRediT authorship contribution statement

Guang Zeng: Methodology, Investigation, Formal analysis, Writing - original draft, Writing - review & editing. **Yijun Zhao:** Methodology, Resources. **Yongtie Cai:** Formal analysis, Writing - review & editing. **Zhimin Zheng:** Writing - review & editing. **Zhenwei Li:** Writing - review & editing. **Mingchen Xu:** Writing - review & editing. **Wenming Yang:** Supervision.

Declaration of Competing Interest

The authors declare that they have no known competing financial interests or personal relationships that could have appeared to influence the work reported in this paper.

Acknowledgement

The authors acknowledge the technical assistance with experiments from Harbin Institute of Technology and National Engineering Laboratory for Reducing Emissions from Coal Combustion in China.

References

[1] BP Statistical Review of World Energy 2019. https://www.bp.com/content/dam/bp/business-sites/en/global/corporate/pdfs/energy-economics/statistical-review/bp-stats-review-2019-full-report.pdf.

[2] Liu Y, Fan W, Li Y. Numerical investigation of air-staged combustion emphasizing char gasification and gas temperature deviation in a large-scale tangentially fired pulverized-coal boiler. Appl Energy 2016;177:323–34.
[3] Zhao Y, Zeng G, Zhang L, Zhang Y, Sun S, Wei C. Effects of fuel properties on ignition characteristics of parallel-bias pulverized-coal jets. Energy Fuels 2017;31:12804–14.
[4] Zeng G, Sun S, Dong H, Zhao Y, Ye Z, Wei L. Effects of combustion conditions on formation characteristics of particulate matter from pulverized coal bias ignition. Energy Fuels 2016;30:8691–700.
[5] Zhang X, Zhou J, Sun S, Sun R, Qin M. Numerical investigation of low-NOx combustion strategies in tangentially-fired coal boilers. Fuel 2015;142:215–21.
[6] Ma L, Fang Q, Yin C, Wang H, Zhang C, Chen G. A novel corner-fired boiler system of improved efficiency and coal flexibility and reduced NOx emissions. Appl Energy 2019;238:453–65.
[7] Zhang Z, Wu Y, Chen D, Shen H, Li Z, Cai N, et al. A semi-empirical NOx model for LES in pulverized coal air-staged combustion. Fuel 2019;241:402–9.
[8] Ti S, Chen Z, Li Z, Kuang M, Xu G, Lai J, et al. Influence of primary air cone length on combustion characteristics and NOx emissions of a swirl burner from a 0.5 MW pulverized coal-fired furnace with air staging. Appl Energy 2018;211:1179–89.
[9] Liang Z, Chen H, Zhao B, Jia J, Cheng K. Synergetic effects of firing gases/coal blends and adopting deep air staging on combustion characteristics. Appl Energy 2018;228:499–511.
[10] Yang J, Sun R, Sun S, Zhao N, Hao N, Chen H, et al. Experimental study on NOx reduction from staging combustion of high volatile pulverized coals. Part 1. Air staging. Fuel Process Technol 2014;126:266–75.
[11] Munir S, Nimmo W, Gibbs B. The effect of air staged, co-combustion of pulverised coal and biomass blends on NOx emissions and combustion efficiency. Fuel 2011;90:126–35.
[12] Sung Y, Moon C, Eom S, Choi G, Kim D. Coal-particle size effects on NO reduction and burnout characteristics with air-staged combustion in a pulverized coal-fired furnace. Fuel 2016;182:558–67.
[13] Rahat AAM, Wang C, Everson RM, Fieldsend JE. Data-driven multi-objective optimisation of coal-fired boiler combustion systems. Appl Energy 2018;229:446–58.
[14] Zhou K, Lin Q, Hu H, Shan F, Fu W, Zhang P, et al. Ignition and combustion behaviors of single coal slime particles in CO2/O2 atmosphere. Combust Flame 2018;194:250–63.
[15] Khatami R, Levendis YA. An overview of coal rank influence on ignition and combustion phenomena at the particle level. Combust Flame 2016;164:22–34.
[16] Xu K, Wu Y, Wang Z, Yang Y, Zhang H. Experimental study on ignition behavior of pulverized coal particle clouds in a turbulent jet. Fuel 2016;167:218–25.
[17] Smith I. The combustion rates of coal chars: a review. In: editor editors. Symposium (International) on combustion; 1982: Elsevier. p. 1045–1065.
[18] Gururajan V, Wall T, Gupta R, Truelove J. Mechanisms for the ignition of pulverized coal particles. Combust Flame 1990;81:119–32.
[19] Khatami R, Stivers C, Levendis YA. Ignition characteristics of single coal particles from three different ranks in O2/N2 and O2/CO2 atmospheres. Combust Flame 2012;159:3554–68.
[20] Khatami R, Stivers C, Joshi K, Levendis YA, Sarofim AF. Combustion behavior of single particles from three different coal ranks and from sugar cane bagasse in O2/N2 and O2/CO2 atmospheres. Combust Flame 2012;159:1253–71.
[21] Pedel J, Thornock JN, Smith PJ. Large eddy simulation of pulverized coal jet flame ignition using the direct quadrature method of moments. Energy Fuels 2012;26:6686–94.
[22] Yamamoto K, Murota T, Okazaki T, Taniguchi M. Large eddy simulation of a pulverized coal jet flame ignited by a preheated gas flow. Proc Combust Inst 2011;33:1771–8.
[23] Su S, Pohl JH, Holcombe D, Hart J. Techniques to determine ignition, flame stability and burnout of blended coals in pf power station boilers. Prog Energy Combust Sci 2001;27:75–98.
[24] Wang Q, Chen Z, Han H, Zeng L, Li Z. Experimental characterization of anthracite combustion and NOx emission for a 300-MWe down-fired boiler with a novel combustion system: influence of primary and vent air distributions. Appl Energy 2019;238:1551–62.
[25] Zeng G, Sun S, Yang X, Zhao Y, Zhao Z, Ye Z, et al. Effect of the primary air velocity on ignition characteristics of bias pulverized coal jets. Energy Fuels 2017;31:3182–95.
[26] Zhang J, Kelly KE, Eddings EG, Wendt JOL. Ignition in 40kW co-axial turbulent diffusion oxy-coal jet flames. Proc Combust Inst 2011;33:3375–82.
[27] Zeng Z, Zhang T, Zheng S, Wu W, Zhou Y. Ignition and combustion characteristics of coal particles under high-temperature and low-oxygen environments mimicking MILD oxy-coal combustion conditions. Fuel 2019;253:1104–13.
[28] Adeosun A, Xiao Z, Gopan A, Yang Z, Wang X, Li T, et al. Pulverized coal particle ignition in a combustion environment with a reducing-to-oxidizing transition. J Energy Inst 2019;92:693–703.
[29] Adeosun A, Xiao Z, Yang Z, Yao Q, Axelbaum RL. The effects of particle size and reducing-to-oxidizing environment on coal stream ignition. Combust Flame 2018;195:282–91.
[30] Yuan Y, Li S, Li G, Wu N, Yao Q. The transition of heterogeneous–homogeneous ignitions of dispersed coal particle streams. Combust Flame 2014;161:2458–68.
[31] Li T, Niu Y, Wang L, Shaddix C, Løvås T. High temperature gasification of high heating-rate chars using a flat-flame reactor. Appl Energy 2018;227:100–7.
[32] Levendis YA, Joshi K, Khatami R, Sarofim AF. Combustion behavior in air of single particles from three different coal ranks and from sugarcane bagasse. Combust Flame 2011;158:452–65.
[33] Riaza J, Khatami R, Levendis YA, Álvarez L, Gil MV, Pevida C, et al. Single particle ignition and combustion of anthracite, semi-anthracite and bituminous coals in air and simulated oxy-fuel conditions. Combust Flame 2014;161:1096–108.
[34] Liang X, Wang Q, Luo Z, Eddings E, Ring T, Li S, et al. Experimental and numerical investigation on sulfur transformation in pressurized oxy-fuel combustion of pulverized coal. Appl Energy 2019;253:113542.
[35] Dobó Z, Backman M, Whitty KJ. Experimental study and demonstration of pilot-scale oxy-coal combustion at elevated temperatures and pressures. Appl Energy 2019;252:113450.
[36] Clements BR, Zhuang Q, Pomalis R, Wong J, Campbell D. Ignition characteristics of co-fired mixtures of petroleum coke and bituminous coal in a pilot-scale furnace. Fuel 2012;97:315–20.
[37] Hwang S-M, Kurose R, Akamatsu F, Tsuji H, Makino H, Katsuki M. Observation of detailed structure of turbulent pulverized-coal flame by optical measurement: part 2, instantaneous two-dimensional measurement of combustion reaction zone and pulverized-coal particles. JSME Int J Ser B, Fluids Therm Eng 2006;49:1328–35.
[38] Zeng G, Sun S, Zhang W, Zhao Z, Zhao Y. Effects of bias concentration ratio on ignition characteristics of parallel bias pulverized coal jets. Energy Fuels 2017;31:14219–27.
[39] Duan L, Li L, Liu D, Zhao C. Fundamental study on fuel-staged oxy-fuel fluidized bed combustion. Combust Flame 2019;206:227–38.
[40] Syrodoy SV, Kuznetsov GV, Zhakharevich AV, Gutareva NY, Salomatov VV. The influence of the structure heterogeneity on the characteristics and conditions of the coal–water fuel particles ignition in high temperature environment. Combust Flame 2017;180:196–206.
[41] Binner E, Zhang L, Li C-Z, Bhattacharya S. In-situ observation of the combustion of air-dried and wet Victorian brown coal. Proc Combust Inst 2011;33:1739–46.
[42] Rezaei D, Zhou Y, Zhang J, Kelly KE, Eddings EG, Pugmire RJ, et al. The effect of coal composition on ignition and flame stability in coaxial oxy-fuel turbulent diffusion flames. Energy Fuels 2013;27:4935–45.
[43] Liu C, Li Z, Zhao Y, Chen Z. Influence of coal-feed rates on bituminous coal ignition in a full-scale tiny-oil ignition burner. Fuel 2010;89:1690–4.
[44] Liu C, Li Z, Kong W, Zhao Y, Chen Z. Bituminous coal combustion in a full-scale start-up ignition burner: influence of the excess air ratio. Energy 2010;35:4102–6.
[45] Chi T, Zhang H, Yan Y, Zhou H, Zheng H. Investigations into the ignition behaviors of pulverized coals and coal blends in a drop tube furnace using flame monitoring techniques. Fuel 2010;89:743–51.
[46] Molina A, Shaddix CR. Ignition and devolatilization of pulverized bituminous coal particles during oxygen/carbon dioxide coal combustion. Proc Combust Inst 2007;31:1905–12.
[47] Liu Y, Geier M, Molina A, Shaddix CR. Pulverized coal stream ignition delay under conventional and oxy-fuel combustion conditions. Int J Greenhouse Gas Control 2011;5:S36–46.
[48] Goshayeshi B, Sutherland JC. A comparison of various models in predicting ignition delay in single-particle coal combustion. Combust Flame 2014;161:1900–10.
[49] Yuan Y, Li S, Zhao F, Yao Q, Long MB. Characterization on hetero-homogeneous ignition of pulverized coal particle streams using CH∗ chemiluminescence and 3 color pyrometry. Fuel 2016;184:1000–6.
[50] Murphy JJ, Shaddix CR. Combustion kinetics of coal chars in oxygen-enriched environments. Combust Flame 2006;144:710–29.
[51] Zhao F, Li S, Ren Y, Yao Q, Yuan Y. Investigation of mechanisms in plasma-assisted ignition of dispersed coal particle streams. Fuel 2016;186:518–24.
[52] Liu B, Wu Y, Cui K, Zhang H, Matsumoto K, Takeno K. Improvement of ignition prediction for turbulent pulverized coal combustion with EDC extinction model. Fuel 2016;181:1265–72.
[53] Prationo W, Zhang J, Cui J, Wang Y, Zhang L. Influence of inherent moisture on the ignition and combustion of wet Victorian brown coal in air-firing and oxy-fuel modes: part 1: the volatile ignition and flame propagation. Fuel Process Technol 2015;138:670–9.
[54] Riaza J, Khatami R, Levendis YA, Álvarez L, Gil MV, Pevida C, et al. Combustion of single biomass particles in air and in oxy-fuel conditions. Biomass Bioenergy 2014;64:162–74.
[55] Zhu M, Zhang H, Tang G, Liu Q, Lu J, Yue G, et al. Ignition of single coal particle in a hot furnace under normal-and micro-gravity condition. Proc Combust Inst 2009;32:2029–35.
[56] Howard J, Essenhigh R. The mechanism of ignition of pulverized coal. Combust Flame 1965;9:337–9.
[57] Molina A, Murphy JJ, Winter F, Haynes BS, Blevins LG, Shaddix CR. Pathways for conversion of char nitrogen to nitric oxide during pulverized coal combustion. Combust Flame 2009;156:574–87.
[58] Howard JB, Essenhigh RH. Pyrolysis of coal particles in pulverized fuel flames. Ind Eng Chem Process Des Dev 1967;6:74–84.
[59] Chang-dong S. Relationship between the ignition modes and the coal concentrations in coal clounds. Power Syst Eng 1995;3.
[60] Zhou K, Lin Q, Hu H, Hu H, Song L. The ignition characteristics and combustion processes of the single coal slime particle under different hot-coflow conditions in N2/O2 atmosphere. Energy 2017;136:173–84.
[61] Kurose R, Ikeda M, Makino H, Kimoto M, Miyazaki T. Pulverized coal combustion characteristics of high-fuel-ratio coals. Fuel 2004;83:1777–85.
[62] Bar-Ziv E, Saveliev R, Korytnyi E, Perelman M, Chudnovsky B, Talanker A. Evaluation of performance of Anglo-Mafube bituminous South African coal in 550 MW opposite-wall and 575 MW tangential-fired utility boilers. Fuel Process Technol 2014;123:92–106.
[63] K. Kang, Development of high efficiency and low NOx combustion technology, Proceedings of the 2016 LRC User Seminar, Seoul, 2016, pp. 14–18.